Preprint typeset using LaTeX style emulateapj v. 5/2/11

arXiv:1610.07610v1 [astro-ph.GA] 24 Oct 2016

GALACTIC ROTATION IN *GAIA* DR1

Jo Bovy[1]
Department of Astronomy and Astrophysics, University of Toronto, 50 St. George Street, Toronto, ON, M5S 3H4, Canada;
bovy@astro.utoronto.ca
and
Center for Computational Astrophysics, 162 5th Ave, New York, NY 10010, USA

ABSTRACT

The spatial variations of the velocity field of local stars provide direct evidence of Galactic differential rotation. The local divergence, shear, and vorticity of the velocity field—the traditional Oort constants—can be measured based purely on astrometric measurements and in particular depend linearly on proper motion and parallax. I use data for 304,267 main-sequence stars from the *Gaia* DR1 Tycho-*Gaia* Astrometric Solution to perform a local, precise measurement of the Oort constants at a typical heliocentric distance of 230 pc. The pattern of proper motions for these stars clearly displays the expected effects from differential rotation. I measure the Oort constants to be: $A = 15.3 \pm 0.4 \pm 0.5\,(\mathrm{syst.})\,\mathrm{km\ s^{-1}\,kpc^{-1}}$, $B = -11.9 \pm 0.4\,\mathrm{km\ s^{-1}\,kpc^{-1}}$, $C = -3.2 \pm 0.4\,\mathrm{km\ s^{-1}\,kpc^{-1}}$ and $K = -3.3 \pm 0.6\,\mathrm{km\ s^{-1}\,kpc^{-1}}$, where the systematic uncertainty in A is due to its uncertain correction for the asymmetric drift. These measurements imply local values for the rotational frequency of $\Omega_0 = 27.1 \pm 0.5 \pm 0.5\,(\mathrm{syst.})\,\mathrm{km\ s^{-1}\,kpc^{-1}}$, for the slope of the rotation curve of $-3.4 \pm 0.6 \pm 0.5\,(\mathrm{syst.})\,\mathrm{km\ s^{-1}\,kpc^{-1}}$, and for the circular velocity of $219 \pm 4 \pm 4\,(\mathrm{syst.})\,\mathrm{km\ s^{-1}}$.

Subject headings: Galaxy: disk — Galaxy: fundamental parameters — Galaxy: kinematics and dynamics — stars: kinematics and dynamics — solar neighborhood

1. INTRODUCTION

Determining the rotation of the Milky Way's disk is difficult, because our vantage point is corotating with the local stars. As first pointed out by Oort (1927) and generalized by Ogrodnikoff (1932), the local rotational frequency and the local change in the circular velocity can be determined from the pattern of line-of-sight velocities and proper motions of nearby stars as a function of Galactic longitude l. Expanding the Milky Way's in-plane velocity field to first order in heliocentric distance in an axisymmetric velocity field, the azimuthal shear and vorticity contribute $\cos 2l$, $\sin 2l$, and constant terms to the mean proper-motion and line-of-sight velocity, which can be distinguished from the $\cos l$ and $\sin l$ pattern due to the Sun's peculiar motion with respect to nearby stars. Going beyond the axisymmetric approximation, the radial shear and divergence contribute similar $\cos 2l$, $\sin 2l$, and constant terms. The four first-order terms (azimuthal and radial shear, vorticity, and divergence) are known as the Oort constants. Measurements of these constants provided the first strong evidence that the Milky Way is rotating differentially with a close-to-flat rotation curve (Oort 1927).

Recently, the best measurements of the Oort constants have used Cepheids to investigate the velocity field on large scales ($> 1\,\mathrm{kpc}$) with a kinematically-cold stellar tracer population (e.g., Feast & Whitelock 1997; Metzger et al. 1998). Because the relative contribution to the velocity pattern from the Sun's peculiar motion to that from Galactic rotation diminishes as the inverse of the distance, the intrinsic velocity field can be more easily determined from such large-scale observations. However, higher-order contributions to the velocity field become important at large distances and the derived values for the Oort constants may not reflect their local value, especially because the local velocity distribution appears to be strongly shaped by non-axisymmetric motions (Dehnen 1998). Local measurements require large stellar samples with good velocity measurements. Olling & Dehnen (2003) attempted a local measurement using proper motions from the Tycho-2 catalog (Høg et al. 2000) that was complicated by the unknown distance distribution at different l, which produces spurious terms in the velocity pattern that are difficult to distinguish from the effects of Galactic rotation.

The *Gaia* mission (Gaia Collaboration et al. 2016a) has recently released its first set of data, including parallaxes and proper motions for about 2 million Tycho-2 stars as part of the Tycho-*Gaia* Astrometric Solution (TGAS, Michalik et al. 2015; Gaia Collaboration et al. 2016b; Lindegren et al. 2016). This large set of astrometric measurements allow the first truly local precise measurement of the Oort constants as discussed in § 2. I describe the data used in this paper in detail in § 3 and the measurement of the Oort constants in § 4. I discuss the results in § 5.

The Oort constants are defined based on the velocity field of (hypothetical) closed orbits. Due to heating by spiral structure and molecular-cloud interactions, stellar orbits are not closed and a range of peri- and apogalacticons are present at the solar radius for any stellar population. Therefore, the mean velocity field does not coincide with that for closed orbits and the measured Oort constants are different from the true Oort constants. I will refer to the "Oort constants" throughout this paper, but it should be understood that the data always measure the Oort constants for the given stellar population. Corrections to the measured Oort constants to bring them closer to the true Oort constants are discussed in § 4.

[1] Alfred P. Sloan Fellow

2. ASTROMETRIC MEASUREMENTS OF THE OORT CONSTANTS

The Oort constants may be measured from the longitudinal and latitudinal proper motions of stars near the Sun. To first order in an expansion of the velocity field in distance from the Sun, we have that the proper motions of stars with parallaxes ϖ depends on (l, b) as

$$\begin{aligned}\mu_l(l) =&(A\,\cos 2l - C\,\sin 2l + B)\,\cos b \\ &+ \varpi\,(u_0\,\sin l - v_0\,\cos l) + \text{scatter}\,,\end{aligned} \tag{1}$$

and

$$\begin{aligned}\mu_b(l) =& -(A\,\sin 2l + C\,\cos 2l + K)\,\sin b\,\cos b \\ &+ \varpi\,[(u_0\,\cos l + v_0\,\sin l)\,\sin b - w_0\,\cos b] + \text{scatter}\,,\end{aligned} \tag{2}$$

where (u_0, v_0, w_0) is the Sun's motion with respect to the stellar population and

$$2A = \frac{\bar{v}_\phi}{R_0} - \left.\frac{\partial \bar{v}_\phi}{\partial R}\right|_{R_0} - \frac{1}{R_0}\left.\frac{\partial \bar{v}_R}{\partial \phi}\right|_{R_0}\,, \tag{3}$$

$$2B = -\frac{\bar{v}_\phi}{R_0} - \left.\frac{\partial \bar{v}_\phi}{\partial R}\right|_{R_0} + \frac{1}{R_0}\left.\frac{\partial \bar{v}_R}{\partial \phi}\right|_{R_0}\,, \tag{4}$$

$$2C = -\frac{\bar{v}_R}{R_0} + \left.\frac{\partial \bar{v}_R}{\partial R}\right|_{R_0} - \frac{1}{R_0}\left.\frac{\partial \bar{v}_\phi}{\partial \phi}\right|_{R_0}\,, \tag{5}$$

$$2K = \frac{\bar{v}_R}{R_0} + \left.\frac{\partial \bar{v}_R}{\partial R}\right|_{R_0} + \frac{1}{R_0}\left.\frac{\partial \bar{v}_\phi}{\partial \phi}\right|_{R_0}\,, \tag{6}$$

are the Oort constants. In these expressions, $(\bar{v}_\phi, \bar{v}_R)$ is the mean rotational and radial velocity, respectively, of the stellar population in Galactocentric cylindrical coordinates with the Sun at $(R, \phi) = (R_0, 0)$ (see Olling & Dehnen 2003 for an elegant derivation of these relations). In an axisymmetric Galaxy, azimuthal derivatives as well as $\bar{v}_R$ are zero, such that $C = K = 0$ and A and B provide direct measurements of the angular rotation frequency $\Omega_0 = V_c/R_0$ at the Sun and the local slope of the rotation curve $\partial V_c/\partial R$.

It is clear from the expressions in equations (1) and (2) that the Oort constants can be measured purely based on astrometric quantities $(l, b, \varpi, \mu_l, \mu_b)$. All of the astrometric quantities appear in a linear fashion and therefore are well behaved. For example, it is unnecessary to invert the parallax to obtain a distance for the measurement of the Oort constants.

3. DATA

I employ parallaxes and proper motions from the *Gaia* DR1 TGAS catalog, which have typical uncertainties of 0.3 mas and 1 mas yr^{-1}. I only consider the 450,278 TGAS sources with relative parallax uncertainties less than 10 % and with inverse parallaxes less than 500 pc to select a local sample. In order to separate stellar populations into kinematically colder and warmer populations, I use matched photometry from APASS (Henden et al. 2012) for the 355,753 stars with APASS photometry to construct the $(B-V, M_V)$ color–magnitude diagram displayed in Figure 1. I select main-sequence stars using the cuts shown in this figure, which creates a sample of 315,946 stars.

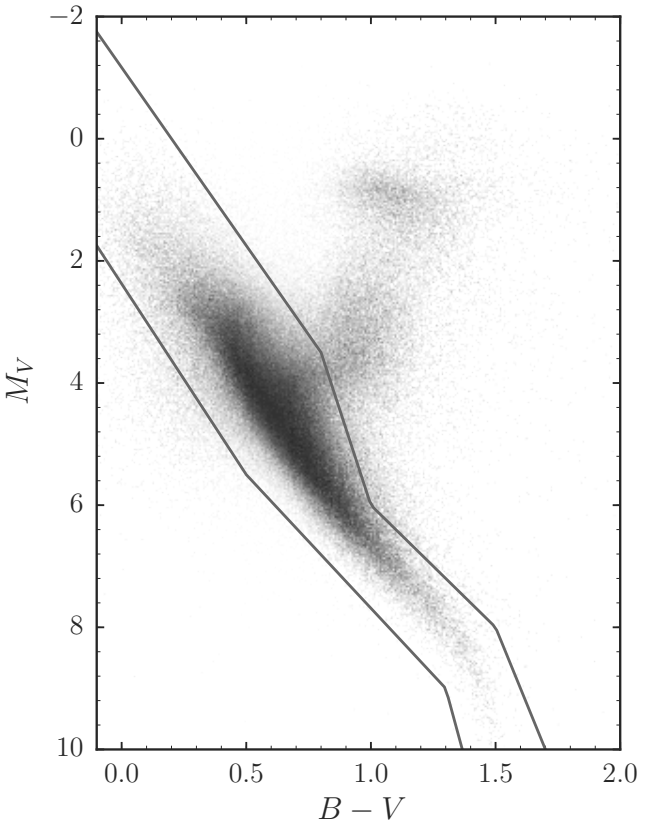

FIG. 1.— Color–magnitude diagram for 355,753 TGAS stars with relative parallax uncertainties less than 10 % within 500 pc that have (B, V) photometry from APASS. The gray curves indicate the cuts that are employed to select the 315,946 main-sequence stars that are used in this paper.

For this sample, I convert the proper motions in equatorial coordinates to Galactic coordinates and propagate the proper-motion uncertainty covariance matrix through this transformation as well. Proper motions in mas yr^{-1} are converted to units of km s^{-1} kpc^{-1} by multiplying them by 4.74047. In what follows, I ignore the correlation between the measurements of the parallax and the Galactic proper motions, because the scatter in the proper motions is dominated by intrinsic scatter (the intrinsic scatter is ≈ 150 km s^{-1} kpc^{-1} due to the small distance range of the sample versus typical measurement uncertainties $\lesssim 5$ km s^{-1} kpc^{-1}). Decorrelating the parallax and proper motion errors by adding random, uncorrelated noise that is four times larger than the formal uncertainties gives changes in the inferred Oort constants below $\lesssim 0.2$ km s^{-1} kpc^{-1}.

4. MEASUREMENT OF THE OORT CONSTANTS

I fit the model in equations (1) and (2) to the data sliced in 0.2 mag bins in $B - V$ using as free parameters $(A, B, C, K, u_0, v_0, w_0)$ and two free parameters describing the Gaussian scatter in (μ_l, μ_b). The parameters A, C, u_0 and v_0 are constrained by both components of the proper motions; fitting them separately to μ_l and μ_b gives consistent results for all four of these. I determine the uncertainty in the best-fit parameters using Markov

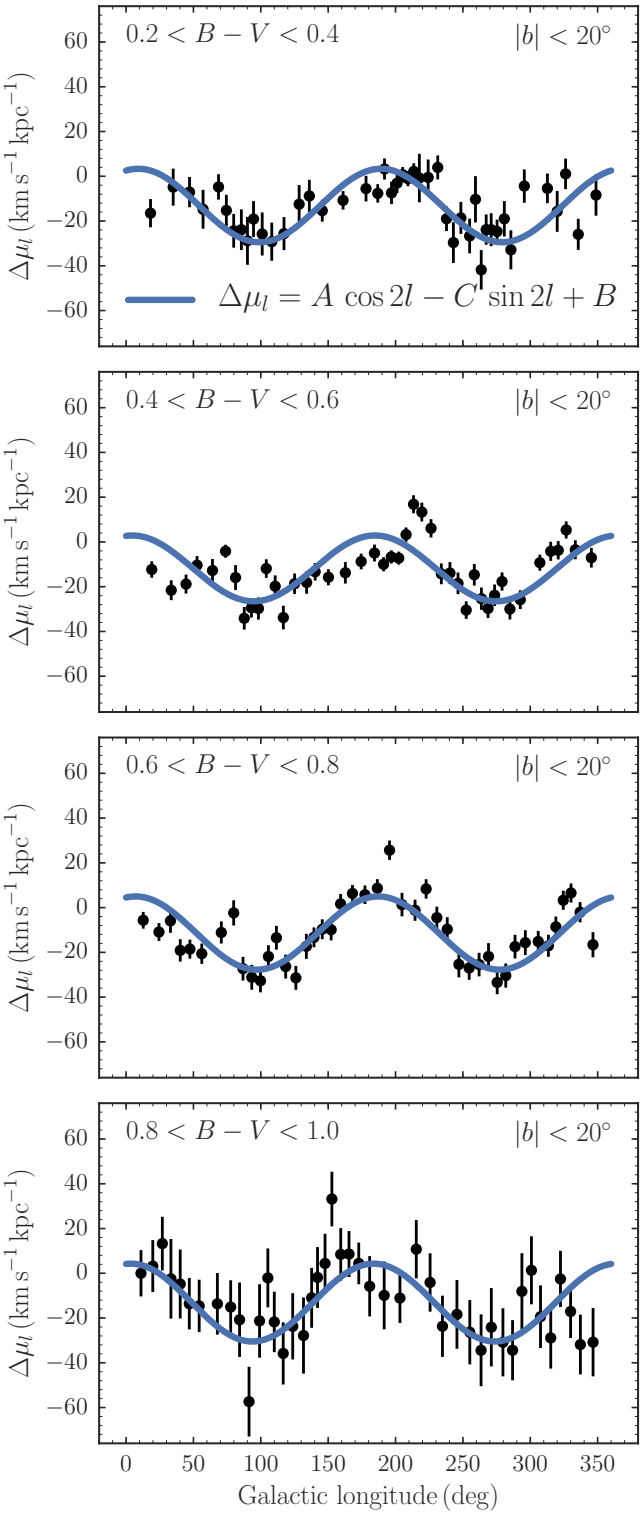

FIG. 2.— Comparison between the observed mean proper motion in Galactic longitude corrected for the solar motion (see equations [7]) as a function of l and the best-fit model for the four main color bins used in the analysis. The data clearly display the expected signatures due to the differential rotation of the Galactic disk. The agreement between the model and the data is good.

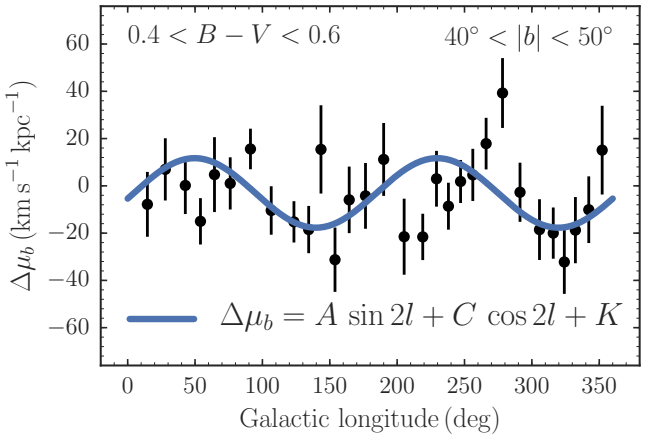

FIG. 3.— Same as Figure 2, but for the proper motion in Galactic latitude for a single color bin with many stars at the intermediate latitudes where Galactic rotation is clearest. The proper motion is corrected for the solar motion (see equations [8]). The data displays the expected $\sin 2l$ behavior due to differential rotation and the non-zero mean offset shows that the local divergence is non-zero due to non-axisymmetric motions.

Chain Monte Carlo with flat priors on all parameters. Note that all parameters except for the scatter terms are linear parameters whose probability distribution at fixed scatter could be obtained analytically, but because we need to fit for the non-linear scatter parameters I do not make use of this simplification.

The best-fitting model to four color bins is compared to the μ_l data in Figure 2. The observed proper motions in this figure have been corrected for the solar motion (u_0, v_0) using the best-fit parameters—because the solar motion is the dominant effect on $\mu_l(l)$ that obscures the Galactic rotation contribution—as follows

$$\Delta\mu_l(l) = (\mu_l - \varpi\,[u_0\,\sin l + v_0\,\cos l])\,/\,\cos b\,, \quad (7)$$

such that the mean $\Delta\mu_l(l) = A\,\cos 2l - C\,\sin 2l + B$. The data is binned to display the mean $\Delta\mu_l(l)$ because of the large scatter of individual data points. Because of the $1/\cos b$ correction, I only show stars with $|b| < 20°$ in Figure 2 that are most valuable to the inference, even though stars at all b are used in the fit.

The proper motion in Galactic latitude is much more tenuously related to the parameters of Galactic rotation because of the $\sin b\,\cos b$ factor in equations (2). Therefore, I only compare the data and the model in Figure 3 for the single $B - V$ bin where enough stars at intermediate b are present to allow for a straightforward data–model comparison. Similar to Figure 2, the proper motion in Figure 3 is corrected for the solar motion as follows

$$\Delta\mu_b(l) = -\,(\mu_b - \varpi\,[(u_0\,\cos l + v_0\,\sin l)\,\sin b - w_0\,\cos b])\,/(\sin b\cos b)\,, \quad (8)$$

such that the mean $\Delta\mu_b(l) = A\,\sin 2l + C\,\cos 2l + K$. The data is again binned to display the mean trend and I restrict the sample to stars with $40° < |b| < 50°$, even though stars at all b are used in the fit.

Overall the data display good agreement with the simple first-order velocity model in both $\mu_l(l)$ and $\mu_b(l)$. The posterior probability distribution for the Oort and solar-

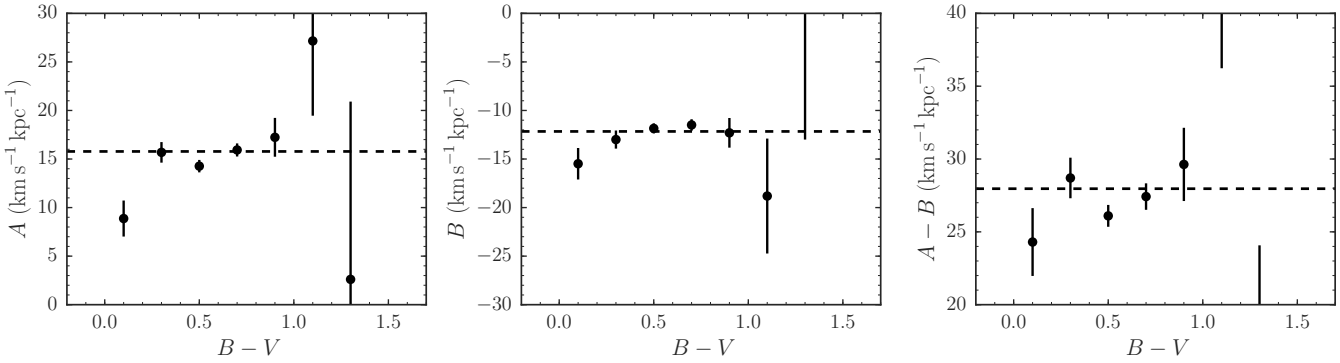

FIG. 4.— Measurements of A, B, and $A-B$ from the TGAS sample for different color bins. The measured values from different color bins agree well, except for the bluest, youngest stars which may be affected by streaming motions at birth. The dashed line in each panel indicates the combined measurement from the four color bins blueward of $B-V=1$ (except for the bluest bin.

motion parameters displays no correlations among any of the parameters, as expected from the full and close to uniform coverage in l of the stars in the TGAS sample.

Figure 4 shows the measurements of A, B, and $A-B$, which is equal to the rotational frequency Ω_0 if the Galaxy were axisymmetric, as a function of $B-V$. The different color bins display excellent agreement with each other, except for the very bluest stars, which are likely affect by residual streaming motions from birth. I combine the four bins blueward of $B-V=1$ (except for the bluest bin) which contain the majority of the stars in the sample (304,267 out 315,946) to obtain a single value of the Oort constants. The combined measurements are: $A = 15.3\pm0.4\,\mathrm{km\ s^{-1}\,kpc^{-1}}$, $B=-11.9\pm0.4\,\mathrm{km\ s^{-1}\,kpc^{-1}}$ as well as $A-B=27.1\pm0.5\,\mathrm{km\ s^{-1}\,kpc^{-1}}$ and $-(A+B)=-3.4\pm0.6\,\mathrm{km\ s^{-1}\,kpc^{-1}}$.

Because stars are not on closed orbits, their mean velocity and the gradients of their mean velocities are not equal to those for the closed orbits that technically define the true Oort constants. It can be shown that the deviation from the true Oort constants is proportional to the asymmetric drift, with a factor of $1/h_\sigma$ and of $(1-R/h_\sigma)/R$ for A and B, respectively, where h_σ is the exponential radial scale length of the radial velocity dispersion (Bovy 2015). Assuming that the solar motion in v with respect to a closed orbit is $\tilde{v}_0 = 12.24\,\mathrm{km\ s^{-1}}$ (Schönrich et al. 2010), the asymmetric drift $v_0-\tilde{v}_0$ for all of the main $B-V$ populations that I consider is $\lesssim 10\,\mathrm{km\ s^{-1}}$, such that the correction to B is negligible for any reasonable h_σ. Fitting a linear relation between A and the asymmetric drift for the four main $B-V$ bins finds a slope that has the wrong sign compared to the theoretical prediction and a corresponding best estimate of the true A of $15.1\,\mathrm{km\ s^{-1}\,kpc^{-1}}$. Forcing the correction to be $(v_0-\tilde{v}_0)/h_\sigma$ with $h_\sigma=8\,\mathrm{kpc}$ gives $A=16.1\pm0.4\,\mathrm{km\ s^{-1}\,kpc}$. Because we do not see the expected trend between A and the asymmetric drift, I therefore assign a systematic uncertainty of $0.5\,\mathrm{km\ s^{-1}\,kpc^{-1}}$ to the measurement of A.

The measurements of C and K are displayed in Figure 5. Like for A and B, the measurements of C and K in different color bins agree with each other, although the formal combined uncertainty is again less than half of the scatter between the different measurements and I again use the latter as a conservative uncertainty estimate. The measurements are: $C=-3.2\pm0.4\,\mathrm{km\ s^{-1}\,kpc^{-1}}$ and $K=-3.3\pm0.6\,\mathrm{km\ s^{-1}\,kpc^{-1}}$. The reason that the uncertainty in K is larger than that in the other parameters is that it can only be determined from the behavior of $\mu_b(l)$. I also find that $K+C=\frac{\partial\bar{v}_R}{\partial R}\big|_{R_0} = -6.6\pm0.7\,\mathrm{km\ s^{-1}\,kpc^{-1}}$. The best-fitting C and K are therefore both significantly non-zero, indicating that the local kinematics is non-axisymmetric. There is no trend in color for either C or K, in disagreement with the previous measurements from Olling & Dehnen (2003).

5. DISCUSSION AND CONCLUSION

I have measured the Oort constants using astrometric measurements for 304,267 local (typical distance of 230 pc) main-sequence stars from the *Gaia* DR1 TGAS catalog:

$$A = \quad 15.3\pm0.4\pm0.5\,(\mathrm{syst.})\,\mathrm{km\ s^{-1}\,kpc^{-1}}\,, \tag{9}$$

$$B = -11.9\pm0.4\,\mathrm{km\ s^{-1}\,kpc^{-1}}\,, \tag{10}$$

$$C = -3.2\pm0.4\,\mathrm{km\ s^{-1}\,kpc^{-1}}\,, \tag{11}$$

$$K = -3.3\pm0.6\,\mathrm{km\ s^{-1}\,kpc^{-1}} \tag{12}$$

These measurements for A and B are in good agreement with those obtained from modeling the Hipparcos proper motions of Cepheids: $A=14.82\pm0.84\,\mathrm{km\ s^{-1}\,kpc^{-1}}$ and $B=-12.37\pm0.64\,\mathrm{km\ s^{-1}\,kpc^{-1}}$ (Feast & Whitelock 1997). The measurement of A is also in good agreement with that measured from the line-of-sight velocities of Cepheids: $A=15.5\pm0.4\pm1.2\,(\mathrm{syst.})\,\mathrm{km\ s^{-1}\,kpc^{-1}}$ (Metzger et al. 1998). Unlike these measurements, the current measurements are based on a sample of stars within a few 100 pc from the Sun and thus truly measure the local velocity field.

The TGAS data also allow a confident measurement of C and K. There are only a few previous measurements of these constants. Olling & Dehnen (2003) measured C from the Tycho-2 proper motions, correcting for the influence of the unknown distance distribution, and found $C=-10\pm2\,\mathrm{km\ s^{-1}\,kpc^{-1}}$ and that C is more negative for older, kinematically-warmer populations. We find that $C=-3.2\pm0.4\,\mathrm{km\ s^{-1}\,kpc^{-1}}$ with no dependence on the color or velocity dispersion of the stellar population. Previous measurements of K using young stars find that it is negative with typical values in the range $-3\,\mathrm{km\ s^{-1}\,kpc^{-1}}$ to $-1\,\mathrm{km\ s^{-1}\,kpc^{-1}}$ (Comeron et al. 1994; Torra et al. 2000) in agreement

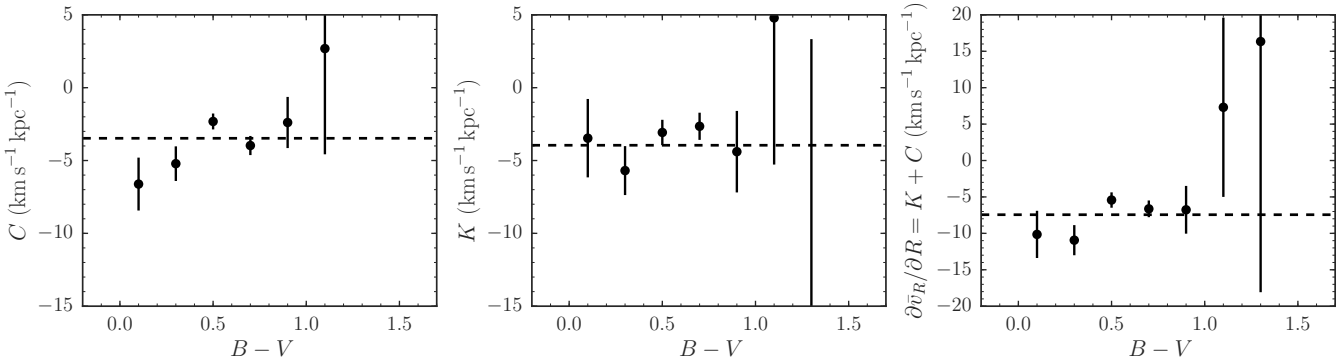

FIG. 5.— Measurements of C, K, and $K + C$ from the TGAS sample for different color bins. The values derived from all of the different color bins show good agreement, with no hint of a trend with color in any of the measurements. The dashed line in each panel indicates the combined measurement from the four color bins blueward of $B - V = 1$ (except for the bluest bin.

with the present measurement. The measurement of $K + C = \frac{\partial \bar{v}_R}{\partial R}\big|_{R_0} = -6.6 \pm 0.7\,\mathrm{km\ s^{-1}\,kpc^{-1}}$ is in good agreement with the measurement of the local mean-radial-velocity gradient from RAVE (Siebert et al. 2011).

That C and K are both non-zero for all color-selected stellar populations provides strong evidence that the local velocity field is significantly affected by non-axisymmetric forces. The localized nature of the measurements using the TGAS sample makes these measurements straightforward constraints on any large-scale non-axisymmetric model such as the bar or spiral arms, in which the Oort constants may simply be evaluated at the position of the Sun and compared to these measurements. For example, for no plausible model with a triaxial bulge or halo in which closed orbits are elliptical do C and K have the same sign (Kuijken & Tremaine 1994; Bovy 2015), such that this model on its own is inconsistent with the current measurements. For an axisymmetric disk plus bar model with the bar's outer Lindblad resonance near the Sun—which can explain the Hercules moving group in the local velocity distribution (Dehnen 2000)—C and K are both negative with $C \approx K \approx -2\,\mathrm{km\ s^{-1}\,kpc^{-1}}$ (computed using `galpy`; Bovy 2015), although kinematically-colder populations in this model respond differently to the bar perturbation and give different C (Minchev et al. 2007), which is not observed in the TGAS data. More sophisticated modeling is required to better interpret the measurements of the Oort constants presented here.

Combining the rotational frequency $\Omega_0 = A - B$ with the current best measurements of R_0 (Chatzopoulos et al. 2015; Boehle et al. 2016) provides a value of the local circular velocity of $219 \pm 4 \pm 4\,(\mathrm{syst.})\,\mathrm{km\ s^{-1}}$.

While the measurements presented here only provide information on the local gravitational field, they may still be usefully employed in the modeling of non-axisymmetric perturbations to the local dynamics. The Oort constants A and B can be used in the sheared sheet approximation to the local dynamics (Spitzer & Schwarzschild 1953; Goldreich & Lynden-Bell 1965) to efficiently determine the effect of different non-axisymmetric forces (e.g., De Simone et al. 2004). This may help elucidate the local non-axisymmetric dynamics from the ≈ 10 million stars within a few 100 pc from the Sun with full velocity measurements in future releases of the *Gaia* data.

I thank Dustin Lang for providing the TGAS-matched APASS data and the 2016 NYC Gaia Sprint participants for stimulating discussions. JB received support from the Natural Sciences and Engineering Research Council of Canada. JB also received partial support from an Alfred P. Sloan Fellowship. The MCMC analyses in this work were run using *emcee* (Foreman-Mackey et al. 2013).

This project was developed in part at the 2016 NYC Gaia Sprint, hosted by the Center for Computational Astrophysics at the Simons Foundation in New York City.

This work has made use of data from the European Space Agency (ESA) mission *Gaia* (`http://www.cosmos.esa.int/gaia`), processed by the *Gaia* Data Processing and Analysis Consortium (DPAC, `http://www.cosmos.esa.int/web/gaia/dpac/consortium`). Funding for the DPAC has been provided by national institutions, in particular the institutions participating in the *Gaia* Multilateral Agreement. This research was made possible through the use of the AAVSO Photometric All-Sky Survey (APASS), funded by the Robert Martin Ayers Sciences Fund.

REFERENCES

Boehle, A., Ghez, A. M., Schödel, R., et al. 2016, ApJ, 830, 17
Bovy, J. 2015, ApJS, 216, 29
Chatzopoulos, S., Fritz, T. K., Gerhard, O., et al. 2015, MNRAS, 447, 948
Comeron, F., Torra, J., & Gomez, A. E. 1994, A&A, 286, 789
Dehnen, W. 1998, AJ, 115, 2384
Dehnen, W. 2000, AJ, 119, 800
De Simone, R., Wu, X., & Tremaine, S. 2004, MNRAS, 350, 627
Feast, M., & Whitelock, P. 1997, MNRAS, 291, 683
Foreman-Mackey, D., Hogg, D. W., Lang, D., & Goodman, J. 2013, PASP, 125, 306
Gaia Collaboration, Prusti, T., de Bruijne, J. H. J., et al. 2016, A&A, in press
Gaia Collaboration, Brown, A. G. A., Vallenari, A., et al. 2016, A&A, in press
Goldreich, P. & Lynden-Bell, D. 1965, MNRAS, 130, 125
Henden A. A., Levine S. E., Terrell D., Smith T. C., & Welch D., 2012, JAVSO, 40, 430
Høg, E., Fabricius, C., Makarov, V. V., Urban, S., Corbin, T., Wycoff, G., Bastian, U., Schwekendiek, P., Wicenec, A., 2000, A&A, 355, 27
Kuijken, K. & Tremaine, S. 1994, ApJ, 421, 178

Lindegren, L., Lammers, U., Bastian, U., et al. 2016, A&A, in press
Metzger, M. R., Caldwell, J. A. R., & Schechter, P. L. 1998, AJ, 115, 635
Michalik, D., Lindegren, L., Hobbs, D., 2015, A&A, 574, 115
Minchev, I., Nordhaus, J., & Quillen, A. C. 2007, ApJ, 664, L31
Ogrodnikoff, K. 1932, ZAp, 4, 190
Olling, R. P. & Dehnen, W. 2003, ApJ, 599, 275
Oort, J. H. 1927, Bull. Astron. Inst. Netherlands, 3, 275
Schönrich, R., Binney, J., & Dehnen, W. 2010, MNRAS, 403, 1829
Siebert, A., Famaey, B., Minchev, I., et al. 2011, MNRAS, 412, 2026
Spitzer, L., Jr. & Schwarzschild, M. 1953, ApJ, 118, 106
Torra, J., Fernández, D., & Figueras, F. 2000, A&A, 359, 82